Magnetic Prandtl Number Dependence of the Kinetic-to-Magnetic Dissipation Ratio

Presented by Andrés Cathey

Axel Brandenburg

KTH Royal institute of Technology and Stockholm University

2014

Overview

Overview

- Electrically conducting fluids.
  - Plasmas.
  - Liquid metals.
  - Electrolytes.

- Electrically conducting fluids.
  - Plasmas.
  - Liquid metals.
  - Electrolytes.
- Moving ρ generate currents.

- Electrically conducting fluids.
  - Plasmas.
  - Liquid metals.
  - Electrolytes.
- Moving ρ generate currents.
- Ampére's law: $\boldsymbol{\nabla} \times \mathbf{B} = \mu_0 \mathbf{J}$.

Magnetohydrodynamics

What exactly is MHD?

- Electrically conducting fluids.
  - Plasmas.
  - Liquid metals.
  - Electrolytes.
- Moving ρ generate currents.
- Ampére's law: $\boldsymbol{\nabla} \times \mathbf{B} = \mu_0 \mathbf{J}$.
- Faraday's law: $\boldsymbol{\nabla} \times \mathbf{E} = -\partial_t \mathbf{B}$.

Navier-Stokes equations

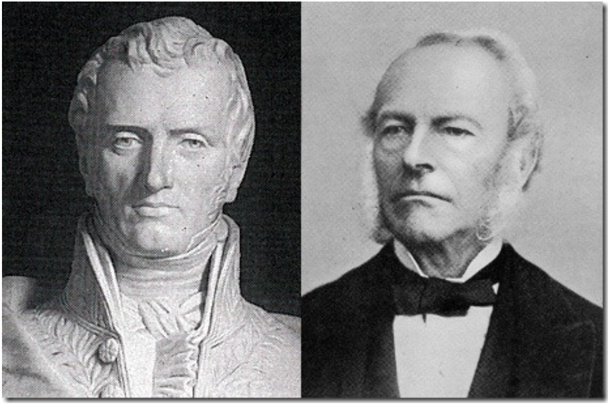

Maxwell equations

Maxwell equations

$$\nabla \cdot E = \frac{\rho}{\varepsilon_0}$$

$$\nabla \cdot B = 0$$

$$\nabla \times E = -\frac{\partial B}{\partial t}$$

$$\nabla \times B = \mu_0 J + \mu_0 \varepsilon_0 \frac{\partial E}{\partial t}$$

Numerical simulations

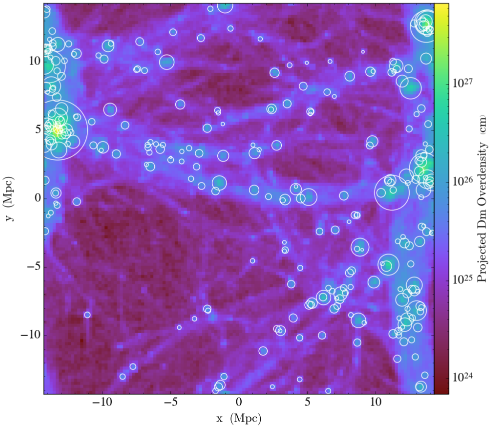

Figure: Cosmological simulation showing dark matter halos.

Numerical simulations

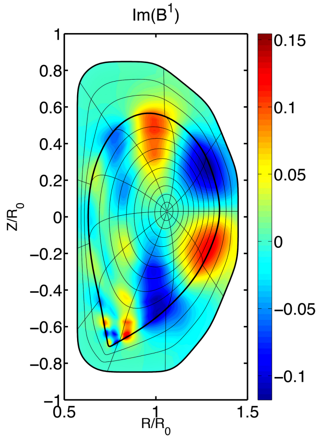

Figure: Radial component of magnetic field amplitude in an unstable n=1 kink mode in DIII-D. MHD Stability code MARS.

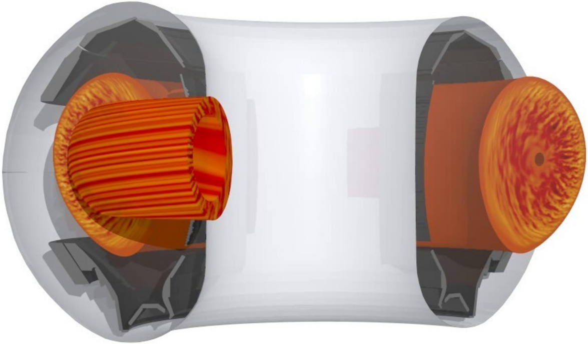

Figure: Snapshot from a numerical simulation of plasma turbulence in the ASDEX Upgrade tokamak with the nonlinear gyrokinetic code GENE. Dr. Jenko

Magnetohydrodynamics

Examples: Magnetic Dynamos - Astrophysical Scales

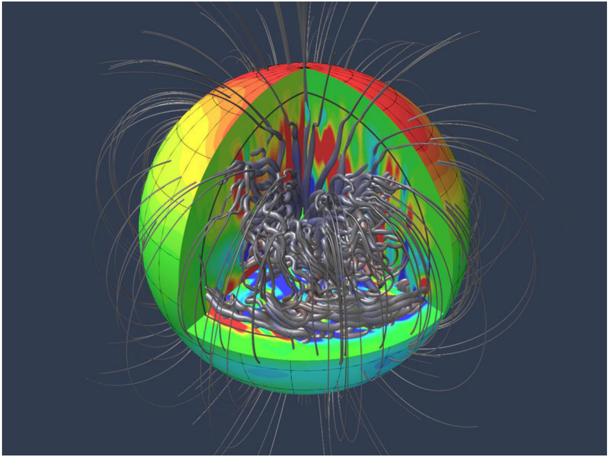

Figure: Jupiter cut open (2014). Dr. Krummheuer & Dr. Wicht

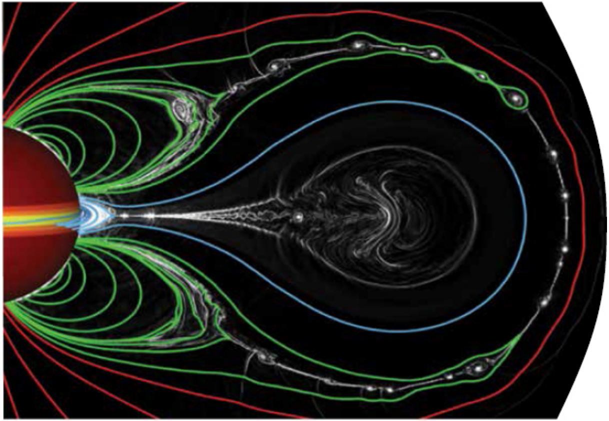

Figure: Ultra-high-resolution numerical simulation of a coronal mass ejection and associated flare. Solar and Space Physics (2010)

Overview

$$Re = \frac{\text{inertial forces}}{\text{viscous forces}} = \frac{u\,L}{\nu}$$

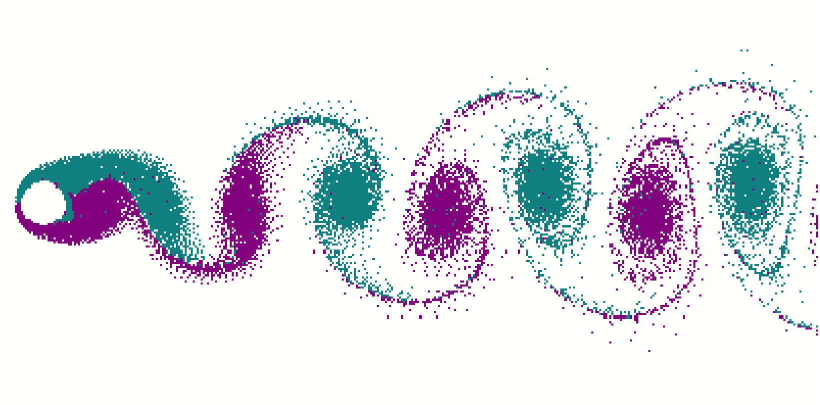

$$Re = \frac{\text{inertial forces}}{\text{viscous forces}} = \frac{u\,L}{\nu}$$

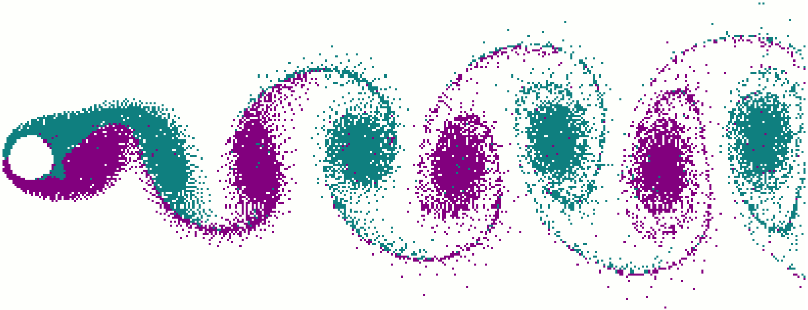

$$Re = \frac{\text{inertial forces}}{\text{viscous forces}} = \frac{u\,L}{\nu}$$

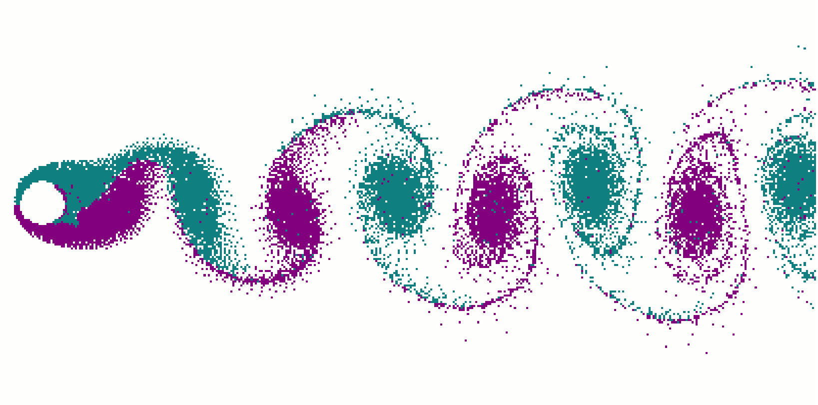

$$Re = \frac{\text{inertial forces}}{\text{viscous forces}} = \frac{u\,L}{\nu}$$

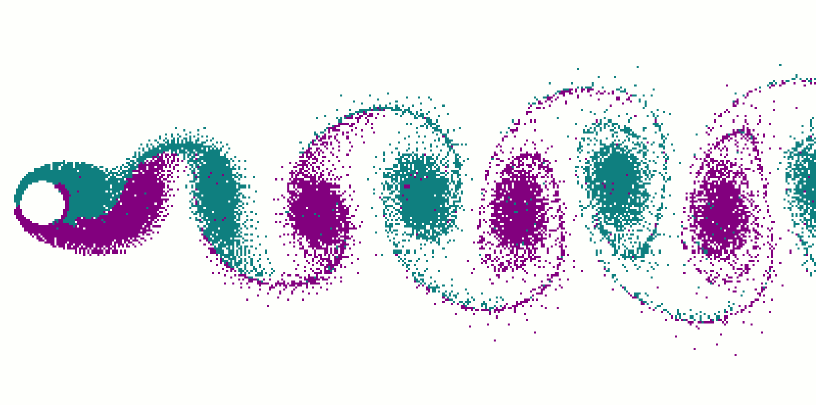

$$Re = \frac{\text{inertial forces}}{\text{viscous forces}} = \frac{u\,L}{\nu}$$

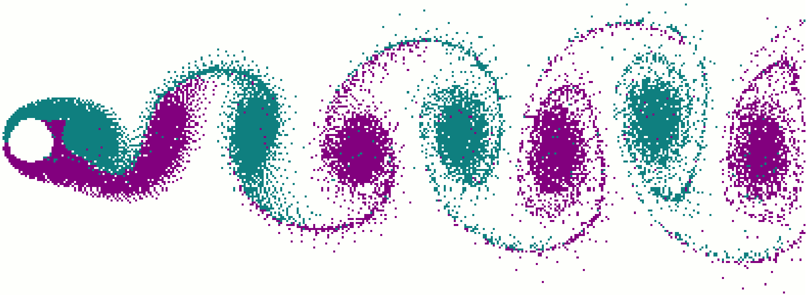

$$Re = \frac{\text{inertial forces}}{\text{viscous forces}} = \frac{u\,L}{\nu}$$

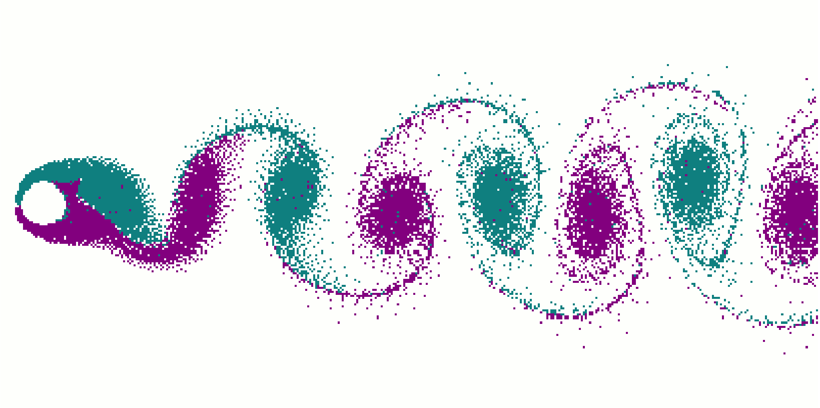

Wikimedia Commons (2014)

Reynolds Numbers and the Magnetic Prandtl Number

Reynolds Number

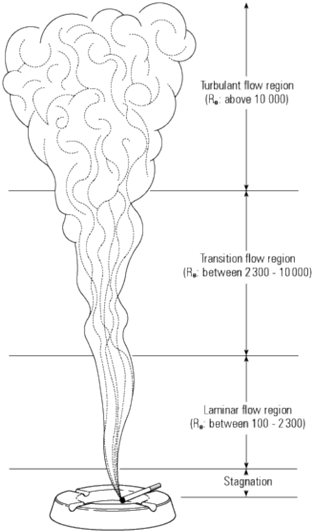

Ideal MHD equations: Perfectly conducting fluids.

$$Re_M = \frac{\text{inertial forces}}{\text{diffusive forces}} = \frac{u\,L}{\eta}$$

$$Pr_M = \frac{Re_M}{Re} = \frac{\nu}{\eta}$$

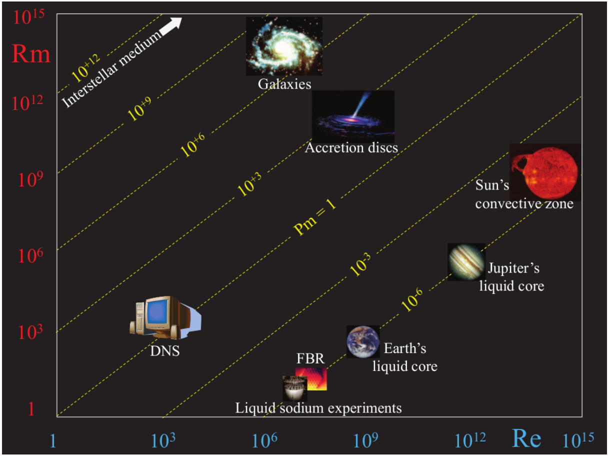

Figure: Map of “typical” objects in the plane (Re, Re_M). Yellow dashed lines are Pr_M isolines. [1].

Overview

Forced MHD turbulence of a gas with isothermal equation of state: $p = \rho c_s^2$.

$$
\begin{aligned}
\frac{D ln\rho}{Dt} &= -\,\boldsymbol{\nabla}\cdot\mathbf{u} \\
\frac{D\mathbf{u}}{Dt} &= -\,c_s^2\boldsymbol{\nabla} ln\rho - 2\boldsymbol{\Omega}\times\mathbf{u} + \mathbf{f} \\
&\quad + \rho^{-1}[\mathbf{J}\times\mathbf{B} + \boldsymbol{\nabla}\cdot(2\nu\rho\boldsymbol{\mathcal{S}})] \\
\frac{\partial\mathbf{A}}{\partial t} &= \mathbf{u}\times\mathbf{B} - \eta\mu_0\mathbf{J}
\end{aligned}
$$

Kinetic and Magnetic energies.

$$\frac{d}{dt}\langle \rho u^2/2\rangle = \langle p\boldsymbol{\nabla}\cdot\mathbf{u}\rangle + \langle \mathbf{u}\cdot(\mathbf{J}\times\mathbf{B})\rangle + \langle \rho\mathbf{u}\cdot\mathbf{f}\rangle - \langle 2\rho\nu\mathcal{S}^2\rangle$$
$$\frac{d}{dt}\langle B^2/2\mu_0\rangle = -\langle \mathbf{u}\cdot(\mathbf{J}\times\mathbf{B})\rangle - \langle \eta\mu_0 J^2\rangle$$

Kinetic and Magnetic energies.

$$\frac{d}{dt}\langle \rho u^2/2\rangle = \langle p\boldsymbol{\nabla}\cdot\mathbf{u}\rangle + \langle \mathbf{u}\cdot(\mathbf{J}\times\mathbf{B})\rangle + \langle \rho\mathbf{u}\cdot\mathbf{f}\rangle - \langle 2\rho\nu\mathcal{S}^2\rangle$$
$$\frac{d}{dt}\langle B^2/2\mu_0\rangle = -\langle \mathbf{u}\cdot(\mathbf{J}\times\mathbf{B})\rangle - \langle \eta\mu_0 J^2\rangle$$

Dissipation rates.

$$\epsilon_K = \langle 2\rho\nu\mathcal{S}^2\rangle, \qquad \epsilon_M = \langle \eta\mu_0 J^2\rangle$$

DNS of Turbulent Dynamos

Governing Equations

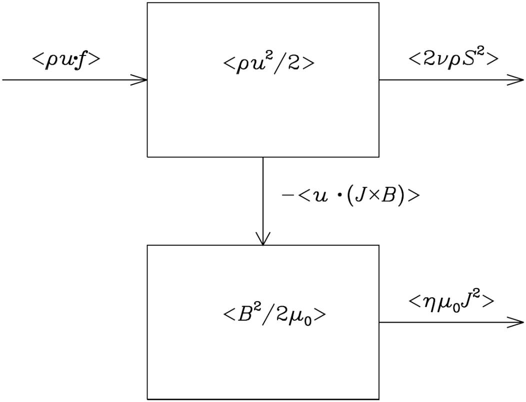

Figure: Flow of energy sketch [2].

Pencil code (NORDITA)

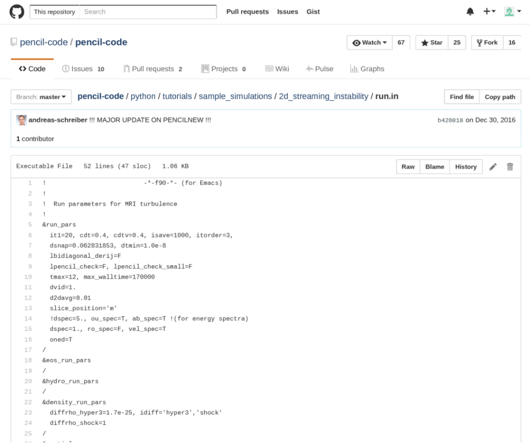

Figure: Snapshot of Pencil-code GitHub repository.

Energy ratio approximately independent on Pr_M.

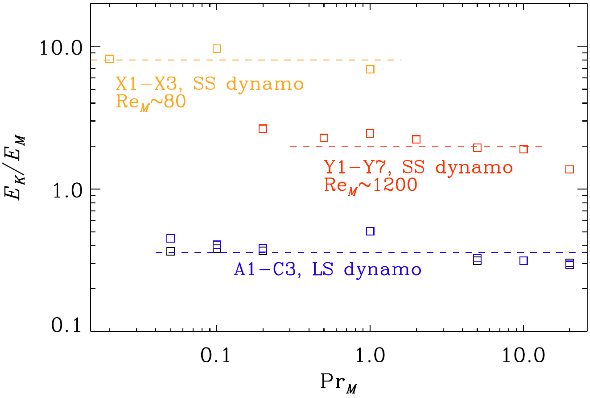

Figure: Energy ratio E_K/E_M dependence on Pr_M for large-scale dynamo (blue) and smal-scale dynamos (orange and red) [2].

Dissipation ratio dependency on Pr_M.

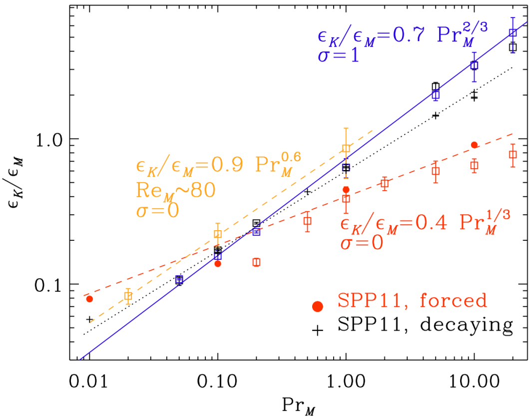

Figure: Dissipation ratio ϵ_K/ϵ_M dependence on Pr_M for non-helical forcing ($\sigma = 0$) and for fully helical forcing ($\sigma = 1$). [2].

Overview

Similar equations than before - same conserved quantities.
Time integration scheme: Adams-Bashforth

Dissipation ratio dependency on Pr_M.

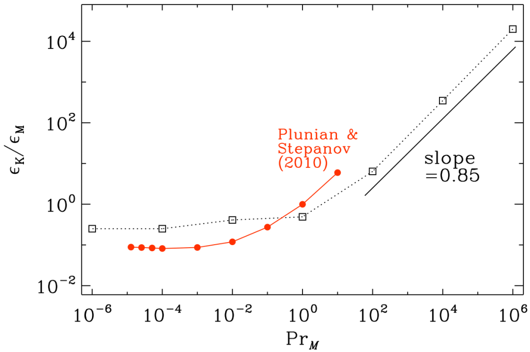

Figure: Dissipation ratio ϵ_K/ϵ_M dependence on Pr_M [2]. Red shows simulations made by Plunian and Stepanov [3].

Neglecting gas pressure:

$$\frac{\partial u}{\partial t} = -uu' - bb' + \tilde{\nu} u''$$
$$\frac{\partial b}{\partial t} = -ub' - bu' + \eta b''$$

Dissipation ratio dependency on Pr_M.

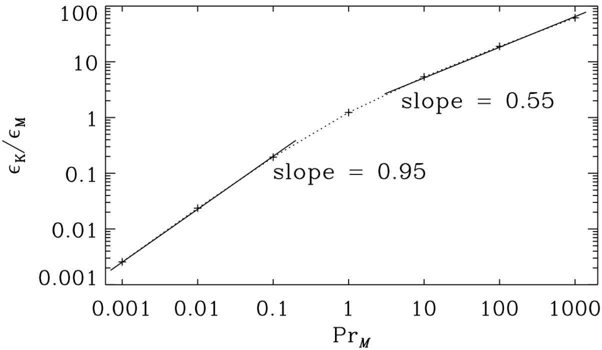

Figure: Dissipation ratio ϵ_K/ϵ_M dependence on Pr_M [2]. Red shows simulations made by Plunian and Stepanov [3].

Overview

Conclusions

1. Obtained relations for the kinetic-to-magnetic dissipation ratio for a broad range of Pr_M values.

Conclusions

1. Obtained relations for the kinetic-to-magnetic dissipation ratio for a broad range of Pr_M values.
2. Discovered scaling laws ($\epsilon_K/\epsilon_M \sim Pr_M^q$) for fully helical and non-helical forcing. Where $q \approx 2/3$ for the former and $q \approx [1/3 - 0.6]$ for the latter.

Conclusions

1. Obtained relations for the kinetic-to-magnetic dissipation ratio for a broad range of Pr_M values.
2. Discovered scaling laws ($\epsilon_K/\epsilon_M \sim Pr_M^q$) for fully helical and non-helical forcing. Where $q \approx 2/3$ for the former and $q \approx [1/3 - 0.6]$ for the latter.
3. Consistent results to previous simulations regarding the kinetic-to-magnetic dissipation ratio were acquired.

References

[1] F. Plunian, R. Stepanov, and P. Frick, "Shell models of magnetohydrodynamic turbulence," *Physics Reports*, vol. 523, no. 1, pp. 1–60, 2013.

[2] A. Brandenburg, "Magnetic prandtl number dependence of the kinetic-to-magnetic dissipation ratio," *The Astrophysical Journal*, vol. 791, no. 1, p. 12, 2014.

[3] F. Plunian and R. Stepanov, "Cascades and dissipation ratio in rotating magnetohydrodynamic turbulence at low magnetic prandtl number," *Physical Review E*, vol. 82, no. 4, p. 046311, 2010.

Dependence on *Re*

Table

Run	$\nu k_1/c_s$	$\eta k_1/c_s$	Re	Re_M	Pr_M	σ	u_{rms}/c_s	b_{rms}/c_s	ϵ_K/ϵ_T	ϵ_M/ϵ_T	C_ϵ	k_ν/k_1	k_η/k_1	res.
A1	5.0×10^{-4}	2.5×10^{-5}	56	1123	20.00	1	0.087	0.158	0.81	0.19	1.83	38	247	1024^3
A2	5.0×10^{-4}	5.0×10^{-5}	57	568	10.00	1	0.088	0.157	0.76	0.24	1.80	37	156	512^3
A3	5.0×10^{-4}	1.0×10^{-4}	57	284	5.00	1	0.088	0.157	0.69	0.31	1.82	36	99	512^3
A4	5.0×10^{-5}	5.0×10^{-5}	587	587	1.00	1	0.091	0.128	0.39	0.61	1.75	179	201	512^3
A5	5.0×10^{-5}	2.5×10^{-4}	606	121	0.20	1	0.094	0.155	0.21	0.79	1.46	150	63	512^3
A6	5.0×10^{-5}	5.0×10^{-4}	594	59	0.10	1	0.092	0.149	0.15	0.85	1.60	139	38	512^3
A7	5.0×10^{-5}	1.0×10^{-3}	581	29	0.05	1	0.090	0.149	0.10	0.90	1.72	125	23	512^3
B1	5.0×10^{-5}	5.0×10^{-5}	587	587	1.00	1	0.091	0.128	0.39	0.61	1.75	179	201	512^3
B2	2.5×10^{-4}	5.0×10^{-5}	117	587	5.00	1	0.091	0.159	0.67	0.33	1.57	60	168	512^3
B3	5.0×10^{-4}	5.0×10^{-5}	57	568	10.00	1	0.088	0.157	0.76	0.24	1.80	37	156	512^3
B4	1.0×10^{-3}	5.0×10^{-5}	27	542	20.00	1	0.084	0.155	0.84	0.16	2.09	23	141	512^3
C1	2.0×10^{-5}	1.0×10^{-4}	1548	310	0.20	1	0.096	0.155	0.19	0.81	1.30	287	124	512^3
C2	2.0×10^{-5}	2.0×10^{-4}	1532	153	0.10	1	0.095	0.149	0.14	0.87	1.41	268	76	512^3
C3	2.0×10^{-5}	4.0×10^{-4}	1516	76	0.05	1	0.094	0.140	0.10	0.90	1.47	248	46	512^3
X1	5.0×10^{-4}	5.0×10^{-4}	56	56	1.00	0	0.113	0.043	0.46	0.54	0.35	28	29	256^3
X2	3.5×10^{-5}	3.5×10^{-4}	864	86	0.10	0	0.121	0.039	0.18	0.82	0.26	159	41	256^3
X3	7.0×10^{-6}	3.5×10^{-4}	4179	84	0.02	0	0.117	0.041	0.08	0.92	0.28	422	42	512^3
Y1	1.0×10^{-3}	5.0×10^{-5}	55	1093	20.00	0	0.082	0.070	0.44	0.56	2.35	16	164	512^3
Y2	5.0×10^{-4}	5.0×10^{-5}	121	1213	10.00	0	0.091	0.066	0.40	0.60	1.79	27	168	512^3
Y3	2.5×10^{-4}	5.0×10^{-5}	245	1227	5.00	0	0.092	0.066	0.38	0.62	1.64	44	167	512^3
Y4	1.0×10^{-4}	5.0×10^{-5}	647	1293	2.00	0	0.097	0.065	0.33	0.67	1.42	85	171	512^3
Y5	5.0×10^{-5}	5.0×10^{-5}	1293	1293	1.00	0	0.097	0.062	0.28	0.72	1.32	135	171	512^3
Y6	2.5×10^{-5}	5.0×10^{-5}	2533	1267	0.50	0	0.095	0.063	0.21	0.79	1.34	210	173	512^3
Y7	1.0×10^{-5}	5.0×10^{-5}	6400	1280	0.20	0	0.096	0.059	0.12	0.88	1.20	356	174	512^3

Shell Models

Energy profiles with shell model

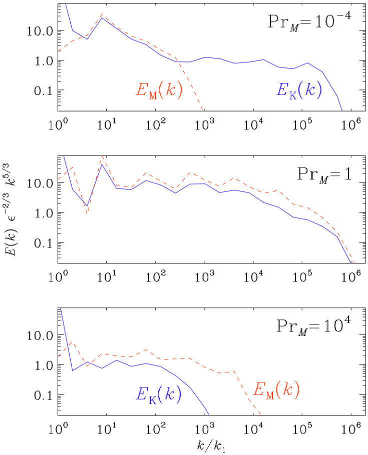

Figure: Compensated time-averaged kinetic and magnetic energy spectra for shell models at three values of Pr_M [2].